

Atomic topography and self-assembly of one-dimensional potassium chains on the InAs(110) surface

Luca Gavioli*

Dipartimento di Matematica e Fisica and INFN, Università Cattolica del Sacro Cuore, Via dei Musei 41, I-25121 Brescia, Italy

Maria Grazia Betti

Dipartimento di Fisica and INFN, Università di Roma "La Sapienza," Piazzale Aldo Moro 2, I-00185 Roma, Italy

Valdis Corradini

Dipartimento di Fisica and INFN, Università di Modena e Reggio Emilia, Via G. Campi 213/A, I-41100 Modena, Italy and INFN National Center on nanoStructures and bioSystems at Surfaces (S³), Via G. Campi 213/A, I-41100 Modena, Italy

Massimo Sancrotti

Dipartimento di Matematica e Fisica and INFN, Università Cattolica del Sacro Cuore, Via dei Musei 41, I-25121 Brescia, Italy and Laboratorio Nazionale TASC-INFN, Strada Statale 14, km. 163.5 Basovizza, I-34012 Trieste, Italy

(Received 24 March 2004; revised manuscript received 22 June 2004; published 24 September 2004)

One-dimensional (1D) potassium chains, obtained on the InAs(110) surface, are studied by scanning tunneling microscopy (STM). The $(2 \times n)$ symmetry in the low energy electron diffraction pattern, becoming a $c(2 \times 6)$ structure at the completion of the first layer, is explained by the various spacing D between alkali chains in the [001] direction. The distribution of D as a function of the chain density suggests the presence of a repulsive interaction among the chains, which drives the self-assembling of the 1D structures. The origin of the interaction is discussed in comparison with the model proposed for the Cs/InAs(110) interface, showing the general validity of the model for this class of chain structures. The atomic structure of an isolated chain is investigated by high-resolution STM images, revealing the asymmetry in the charge density induced by K adatoms and a modification of the As-related charge density of the topmost substrate layer.

DOI: 10.1103/PhysRevB.70.125317

PACS number(s): 68.43.Fg, 68.47.Fg, 73.20.-r, 68.37.Ef

I. INTRODUCTION

A widespread interest in low-dimensional structures is growing, as techniques are becoming available to produce new artificial architectures with regular size and spacing, controlled at the atomic scale. The low dimensionality of such structures is providing a specific field to investigate physical properties different from bulk,¹⁻³ and can be obtained using suitable templates to pattern overlayer growth, like stepped surfaces,⁴⁻⁶ or inducing chain-like reconstructions,⁷⁻⁹ or assembling adsorbates on anisotropic surfaces.¹⁰⁻¹³ The most efficient mechanism is the self-assembling in which mutual interactions of simple building blocks (atoms or molecules) give rise to well-defined and regular structures, with dimensions ranging from few nanometer to hundreds of nanometers.

Cesium adsorbed on III-V(110) semiconductor surfaces is the only alkali metal that has been experimentally observed to form chains oriented along the $[1\bar{1}0]$ direction and extending for tens of nanometers.¹⁰⁻¹⁴ The atomic and electronic structure of the Cs chains is still debated. The Cs/InAs(110) atomic geometry proposed by recent surface x-ray diffraction data,¹⁴ evidences two nonequivalent adsorption sites for Cs adatoms, in agreement with core-level investigations.^{13,15,16} Previous scanning tunneling microscopy (STM) images on Cs/GaAs(110)^{11,12} have been interpreted in terms of the formation of a symmetric zig-zag chain along the $[1\bar{1}0]$ direction, with a single adsorption site for the couple of alkali

adatoms. Such geometry, corresponding to a $c(2 \times 2)$ unit cell, has been the base to justify the insulating nature of the Cs chains^{11,12,17,18} in terms of electron correlation effects.^{19,20} A recent theoretical calculation²¹ proposed an alternative explanation by considering unbalanced charge transfer between the alkali metals and the unoccupied dangling bonds of the substrate, giving rise to a $p(2 \times 2)$ unit cell. The different charge transfer, inducing the splitting of the partially occupied surface band, gives rise to a semiconducting system without including correlation effects,²¹ questioning the validity of the generally accepted explanation of such systems in terms of Mott-Hubbard insulators.¹⁹ In particular, this work predicts a STM image in which only a single electronic cloud is present for K on InAs(110).²¹ Despite extensive investigation of alkali adsorption on III-V substrates, only recently we have shown the possibility to fabricate potassium chains on the InAs(110) surface by optimizing the kinetic growth conditions,²² providing a way to extend the experimental investigations to low-dimensional chains made by a different alkali metal.

The aim of our paper is therefore to present the study of K-induced chains on InAs(110) in order to clarify the atomic structure and symmetry of the alkali chains, and compare to the most recent theoretical hypothesis. This work is showing that the self-organization process is actually taking place also for potassium and can therefore be a general model of alkali chain formation on III-V(110) substrates. STM images on a single chain reveal the twofold symmetry of the electron

charge density distribution due to the K adatoms in the $[1\bar{1}0]$ direction. The modification of the As-related charge density, observed in the vicinity of the chain, and the strong asymmetry in K-related charge density is discussed considering the atomic model and the symmetry of the system.

II. EXPERIMENTAL DETAILS

The InAs(110) single crystal is an *n*-type doped specimen ($n=4 \times 10^{17} \text{ cm}^{-3}$) and the (110) clean surface has been obtained by several cycles of sputtering (Ar^+ , $E_p=600 \text{ eV}$) and annealing at 720 K. The average terrace width of the clean surface observed by STM is about 120 nm. Pure potassium has been evaporated from a well-outgassed SAES Getters alkali metal dispenser on the substrate held at 420 K, with the pressure kept below 2×10^{-10} mbar. In the following, θ_{SAT} is the K saturation coverage, that corresponds to the completion of a second overlayer, estimated from the STM images to be $0.42 \pm 0.07 \text{ ML}$ (with 1 ML defined as two K atoms per surface unit cell).

The STM experiments have been performed at the INFM Nanoscience Laboratory of the Università Cattolica del Sacro Cuore (Brescia, Italy) on an OMICRON STM/SEM/SAM UHV system (base pressure 2.5×10^{-11} mbar), equipped with ancillary facilities for sample preparation and quality control. STM images have been collected at negative sample-to-tip biases ranging from -1.3 V to -2.5 V , in constant current mode ($0.1\text{--}0.3 \text{ nA}$). Tungsten tips have been prepared by chemical etching method in a 2N NaOH solution and subsequently bombarded in ultra high vacuum with high energy electrons (up to 1 keV) to eliminate residual tip contamination. Length scale calibration of images has been performed by comparison to the InAs(110) substrate surface lattice spacing, clearly identifiable in the STM pictures.

III. RESULTS AND DISCUSSION

Symmetry and long-range ordering of the K chains deposited on the InAs(110) surface have been studied by low-energy electron-diffraction (LEED). The LEED patterns for the clean InAs(110) surface and for the K/InAs(110) interface at increasing alkali depositions ($\theta=0.25 \theta_{\text{SAT}}$ and $\theta=0.38 \theta_{\text{SAT}}$) are displayed in Figs. 1(a)–1(c). The twofold symmetry, visible even at low K coverage, is given by the presence of extra-stripes located between the integer order spots of the (1×1) InAs reciprocal unit cell along the $[1\bar{1}0]$ direction. The stripes, extending along the $[001]$ direction, suggest the presence of an *n*-fold symmetry, with *n* decreasing as a function of increasing K coverage. At the completion of the first ordered one-dimensional (1D) chain layer ($\theta=0.39 \theta_{\text{SAT}}$), the stripes merge in definite spots giving rise to a $c(2 \times 6)$ symmetry, as observed in Fig. 1(c).

The evolution of the diffraction pattern is consistent with the atomic topography observed in the STM images, where regular one-dimensional chains are aligned along the $[1\bar{1}0]$ direction, even at low coverage, as shown in Fig. 2(a) for $\theta=0.17 \theta_{\text{SAT}}$. The negative-biased STM image shows the K chains as well as the substrate lattice of As atoms, providing

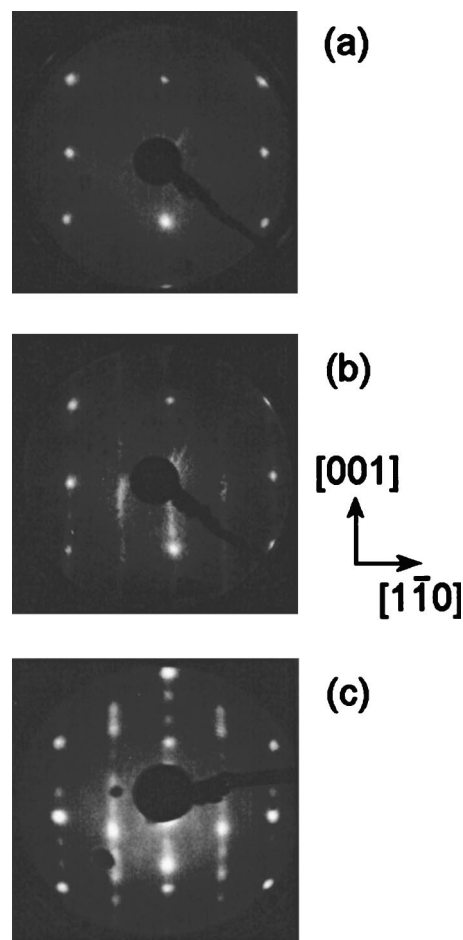


FIG. 1. Low energy electron diffraction patterns taken at 23 eV of primary electron energy for the InAs(110) clean surface (a) and at K coverage of (b) $\theta=0.25 \theta_{\text{SAT}}$, and (c) $\theta=0.4 \theta_{\text{SAT}}$. The potassium is deposited on the InAs(110) surface kept at 420 K temperature. The stripes indicate a twofold periodicity along the $[1\bar{1}0]$ direction and an *n*-fold superstructure along the $[001]$ direction perpendicular to the chains, with *n* decreasing as a function of K chain density until the formation of the $c(2 \times 6)$ periodicity (c).

a simple way of measuring the chain to chain distance (*D*) in terms of the substrate lattice constant a_0 along the $[001]$ direction ($a_0=0.604 \text{ nm}$). In Fig. 2(b) is plotted the height profile of the STM line scan marked in Fig. 2(a) which presents two main peaks, corresponding to the center of two K chains. The distance *D* between the center of the two chains is 10 times a_0 , as well as the distance among other chains is always an integer multiple of a_0 ($D=n \times a_0$). The presence of different values of *D* observed in the STM image at each coverage explains the striped intensity of the LEED pattern observed up to the completion of the first layer (Fig. 1(b)).

By increasing the potassium coverage, the chains density increases up to the completion of the first layer ($\theta=0.39 \theta_{\text{SAT}}$), while the structure of the single chain is not modified (Fig. 3(a)). At the first layer maximum packing (Fig. 3(a)), most of the adjacent chains are shifted with respect to each other by one substrate unit cell in the $[1\bar{1}0]$ direction. Such shift determines the symmetry of the system unit cell at this coverage, suggested in Fig. 3(b). Two equiva-

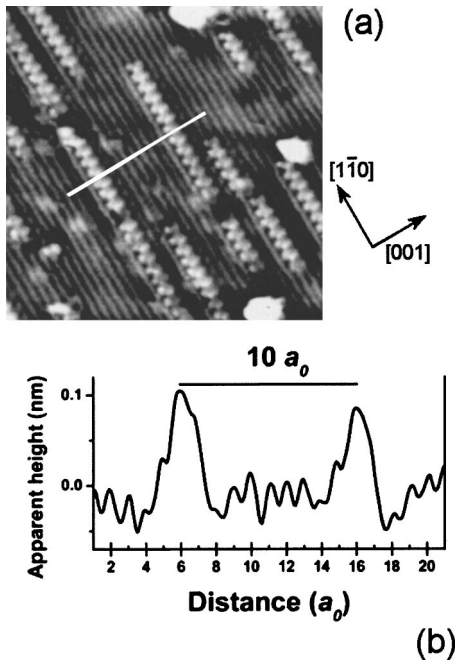


FIG. 2. (a) STM image ($20 \times 20 \text{ nm}^2$) of potassium chains ($\theta = 0.17 \theta_{\text{SAT}}$) deposited on the InAs(110) surface kept at 420 K temperature. Sample-to-tip bias -1.6 V . (b) Line profile taken from the gray line marked in the image. The length is given in integer multiples of the clean substrate surface lattice constant a_0 .

lent maxima of the adjacent chains are found moving by one cell in the $[1\bar{1}0]$ direction and by 3 cells in the $[001]$ direction, i.e., the corner and the center of the unit cell are equivalent, producing a $c(2 \times 6)$ unit cell, which justifies the $c(2 \times 6)$ LEED pattern observed in Fig. 1(c).

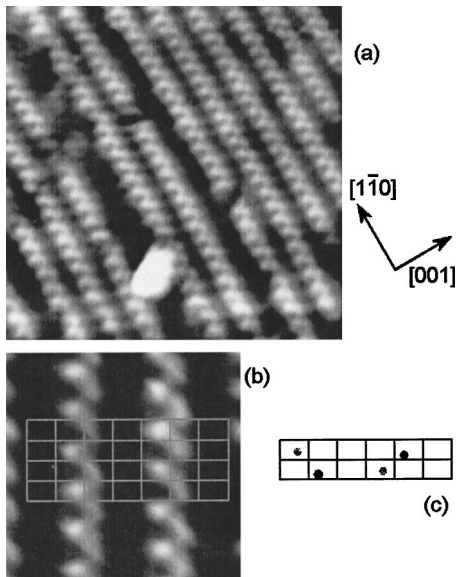


FIG. 3. (a) STM image ($20 \times 20 \text{ nm}^2$) of potassium chains ($\theta = 0.35 \theta_{\text{SAT}}$). Sample-to-tip bias -1.9 V . The minimum chain distance is 1.8 nm . (b) High resolution STM image ($4.7 \times 4.7 \text{ nm}^2$) of two adjacent potassium chains. Sample-to-tip bias -1.6 V . The grid represents the InAs(110) surface unit cell centered on the As atoms. (c) Schematic drawing of the $c(2 \times 6)$ unit cell in which the inequivalent maxima are indicated by closed circles.

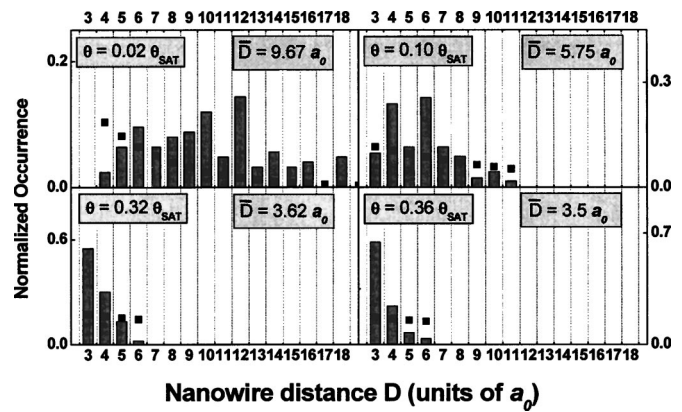


FIG. 4. Statistical distribution of the separation, D , between 1D nanowires along the $[001]$ direction for different K coverage as derived by the STM images. The separation D between chains is always a multiple of the lattice vector $a_0 = 0.604 \text{ nm}$. The exponential distribution corresponding to a random adsorption process is also shown for comparison (squares).

The statistical distribution of the actual chain separation D along the $[001]$ direction, obtained from the STM images, is shown in Fig. 4 for various K coverage, compared with the distribution expected from a random adsorption process (squares). The distance between two adjacent chains has been determined by directly counting the number of substrate unit cells observed between the centers of adjacent chains in the STM images. Each histogram represents a total of 300–400 measurements taken in different areas of the sample surface (each coverage is indicated in the figure). The STM images, considered for the statistical distribution, have a size ranging from 80 nm^2 down to 20 nm^2 . In each histogram the sum of the occurrences is normalized to 1. The mean deviation of the normalized distribution is $2.76 a_0$ at a coverage $\theta = 0.02 \theta_{\text{SAT}}$, $1.55 a_0$ at $\theta = 0.1 \theta_{\text{SAT}}$, $0.65 a_0$ at $\theta = 0.32 \theta_{\text{SAT}}$, and $0.68 a_0$ at $\theta = 0.36 \theta_{\text{SAT}}$. The average distance of each normalized distribution is indicated in each histogram.

The separation D is peaked around $10 a_0$ at $\theta = 0.02 \theta_{\text{SAT}}$, and around $6 a_0$ at $\theta = 0.1 \theta_{\text{SAT}}$, while it drops down to $3 a_0$ before the completion of the first layer. At the saturation of the first layer 95% of the chains is separated by $3 a_0$, corresponding to a coverage of $\theta = 0.39 \theta_{\text{SAT}}$. We never observed lower values of D in many different experiments, indicating that the minimum allowed distance between two K chains is $3 a_0$. It is clear from Fig. 4 that the distribution of the D values at each coverage is always far from the exponential distribution arising from a random process, and that the chains prefer to be separated rather than packed, indicating that chains repel each other in the $[001]$ direction.

In the simple model proposed for Cs adsorption on InAs(110),¹³ the chain repulsion is justified by considering chains of interacting dipoles oriented perpendicular to the surface, maximizing their mutual distance and depolarizing each other. When two chains come close to each other, the dipoles lie in an unfavorable energetic configuration due to the electric field of the adjacent chain. This results in a decrease of the dipole intensity (depolarization), which depends on the chain distance D . If one compares the statistical

distributions for the two alkali metals, the behavior is quite similar, except for the most probable chain distance at the saturation coverage, which is $2 a_0$ for Cs^{13,14} and $3 a_0$ for K, with an average distance $\langle D \rangle$ of 1.5 nm for Cs and 1.8 nm for K.

To quantitatively compare with the Cs/InAs(110) system, we evaluated the variation of the dipole moment per chain unit length δl as a function of D . We can write the dependence of $\delta p(D)$ on chain distance as

$$\delta p(D) = \delta p_0 [1 + (k^* a/D^2)], \quad (1)$$

where α is the alkali metal polarizability ($5.96 \times 10^{-2} \text{ nm}^3$ for atomic Cs and $4.34 \times 10^{-2} \text{ nm}^3$ for atomic K²³) and $k^* = k/\delta l$, where k is a numerical factor depending on the geometrical distribution of the overlayer atoms. Equation (1) is analogous to the Helmholtz equation considering the dipoles arranged along chains. In the case of chains k takes the value $2 \sum_1^\infty 1/n^2 = 3.2$. From the STM images, we evaluate the linear dipole density in the chains, and we assume an average value of one dipole per unit cell, without considering the nonequivalent charge transfer discussed later (in the chain direction $\delta l = 0.425 \text{ nm}$), so that $k^* = 7.49 \text{ nm}^{-1}$. When the interchain distance decreases from $12 a_0$ to $3 a_0$ the dipole moment magnitude is reduced by 8.5% for K and 11% for Cs.¹³ This different reduction of the dipole moment depends on the reduced polarizability of K vs Cs. To evaluate the influence of the polarizability on the chain distance at the saturation of the first layer, we write the repulsive potential energy per chain unit length δl between two dipoles chains at a distance D ,

$$E_p^w = \frac{\delta p_0^2}{2\pi\epsilon_0\delta l} \left(\frac{D}{D^2 + k^* \alpha} \right)^2, \quad (2)$$

in which the dependence on the depolarization effect is explicit. If we replace the polarizability value (α) for Cs with the value for K, keeping constant all the other quantities, the chain distance (D) changes from 1.5 to 1.6 nm, with a variation of 0.1 nm (7%), while the experimental difference between Cs and K is 0.3 nm (20%). Thus the contribution of the atomic polarizability to the chain spacing is just 1/3 of the actual difference. This estimation suggests that other factors contribute to the chain repulsion. In particular, the actual dipole length and hence the dipole moment intensity might be different in Cs and K, due to different geometric positions with respect to the substrate and unequal charge transfer to the empty dangling bonds, caused by the different electronegativity of the two alkali metals. The rather crude model discussed here does not allow a quantitative determination of the contributing factors. However, our data show that the repulsion mechanism is applicable to the K chains on the InAs(110) surface, supporting the presence of such repulsion for any alkali metal adsorbed on III-V substrates and the general validity of the dipole interaction for this class of one-dimensional structures.

A detailed investigation of the atomic geometry is partly hampered by the fact that STM is sensing the charge density distribution in real space rather than the actual geometric position of the atoms (see for instance Ref. 24). Neverthe-

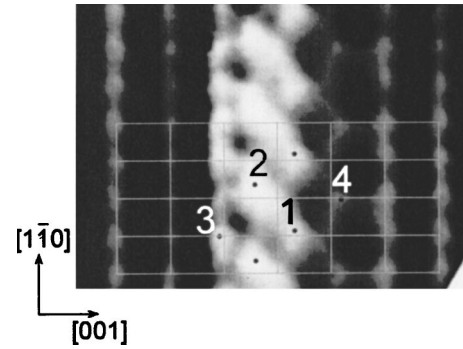


FIG. 5. (a) High resolution STM image ($4.4 \times 3.3 \text{ nm}^2$) of a single K chain. Sample-to-tip bias of -1.5 V . The line grid represents the InAs(110) surface unit cell centered on the As atoms. Maxima of charge density are numbered from 1 to 4.

less, information on the chain symmetry can be extracted from high-resolution STM image shown in Fig. 5(a), where an isolated potassium chain and the substrate lattice As atoms are visible. The chain is extending over two substrate cells in the $[001]$ direction, and presents two main maxima (indicated by dots 1 and 2), periodically repeated along the chain, due to the presence of a couple of K adatoms. Such features justify the twofold symmetry along the $[1\bar{1}0]$ direction observed in the LEED pattern.

The two maxima do not occupy the same position with respect to the substrate unit cell suggesting an nonequivalent charge redistribution among the K adatoms and the In unoccupied bonds. In particular the maximum 1 position is 0.14 nm away from the center of the substrate unit cell in the $[1\bar{1}0]$ direction. Modification of the occupied charge density associated to the As substrate atoms is observed on both sides of the chains, as compared to the clean surface lattice positions, evidenced by the grid (Fig. 5(a)). On the left-hand side of the K chain, the distance of the maximum labeled 3 from the nearest As atom along the $[001]$ direction is reduced by 5% with respect to a_0 . On the right-hand side of the chain, a much stronger reduction (16%) of such distance can be observed for the As-related charge density in position 4. Again, this is consistent with nonequivalent charge transfer from alkali adatoms to the substrate empty In dangling bonds. It is worth noting that the asymmetry of the potassium chains is always present regardless of the tip influence on the images, even if the apparent distribution might change from tip to tip.

The STM images are compatible with the atomic geometry deduced by the surface x-ray diffraction experiment for Cs/InAs(110),¹⁴ where the alkali atoms present two nonequivalent adsorption sites, both positioned close to the unoccupied In dangling bonds: the unbuckling site (maximum 2) and the overbuckling site (maximum 1). Hence the asymmetric shape of the charge density along the chain is probably due to unbalanced charge transfer between each K and the In substrate atoms, leading to the presence of nonequivalent alkali adsorption sites, as suggested in the literature.^{15,16,21,25,26} Such a model accounts for the stronger distortion observed in the STM images on the right-hand side of the alkali chains with respect to the left-hand side.

It is worth noting that the long range order of the nanostructures (the $c(2 \times 6)$ symmetry), is simply generated by the relative shift of two adjacent chains (see Fig. 3), but does not depend on a symmetric or asymmetric charge density distribution. Previous theoretical calculations of the electronic structure have been done using equivalent adsorption sites and charge transfer to the substrate, and hence a $c(2 \times 2)$ unit cell.^{19,20} Only recently a single particle calculation proposed a different framework using a $p(2 \times 2)$ atomic geometry, in which the alkali charge is transferred to one single indium-related dangling bond.²¹ The theoretical STM image, obtained considering charge transfer to a single cation dangling bond, is not consistent with the STM data, suggesting that both alkali adatoms contribute to the electronic charge density distribution of the system.

IV. CONCLUSIONS

We presented an extensive study of the structural properties of K nanochains on the InAs(110) surface. The separation D of the one-dimensional alkali chains is an integer

multiple of the substrate lattice constant a_0 . The different values of D at each coverage explain the $(2 \times n)$ symmetry of the LEED pattern. At the saturation of the first layer we identify a $c(2 \times 6)$ long-range ordered phase, where 95% of the K chains are spaced by $D=3 a_0$. The shift of the chains by one unit cell in the $[1\bar{1}0]$ direction is responsible for the centered symmetry, independently of adsorption sites type. The distribution of D shows that the chains are formed by a self-assembling process, due to a repulsive interaction generated by formation of dipoles perpendicular to the surface. The separation D obtained at the maximum packing of the chains indicates that the intensity of the interaction depends on the alkali metal. Nevertheless, our data prove that the interchain interaction model can be applied to other types of alkali metal adsorbates on III-V(110) substrates.

ACKNOWLEDGMENT

The nanospectroscopy facility in Brescia was funded by INFN under the "Strumentazione Avanzata" programme.

*Author to whom correspondence should be addressed; electronic address: l.gavioli@dmf.unicatt.it

- ¹C. Kim, A. Y. Matsuura, Z. X. Shen, N. Motoyama, H. Eisaki, S. Uchida, T. Tohyama, and S. Maekawa, *Phys. Rev. Lett.* **77**, 4054 (1996).
- ²R. Claessen, M. Sing, U. Schwingenschlöggl, P. Blaha, M. Dressel, and C. S. Jacobsen, *Phys. Rev. Lett.* **88**, 096402 (2002).
- ³L. Perfetti, S. Mitrovic, G. Margaritondo, M. Grioni, L. Forrò, L. Degiorgi, and H. Höchst, *Phys. Rev. B* **66**, 075107 (2002).
- ⁴P. Gambardella, M. Blanc, H. Brune, K. Kuhnke, and K. Kern, *Phys. Rev. B* **61**, 2254 (2000).
- ⁵G. I. Hill, and A. B. Mc Lean, *Phys. Rev. Lett.* **82**, 2155 (1999).
- ⁶P. Segovia, D. Purdie, M. Hengsberger, and Y. Baer, *Nature (London)* **402**, 504 (1999).
- ⁷C. Binns and C. Norris, *J. Phys.: Condens. Matter* **3**, 5425 (1991).
- ⁸E. Bertel and J. Lehman, *Phys. Rev. Lett.* **80**, 1497 (1998).
- ⁹H. H. Weitering, J. Chen, N. J. Di Nardo, and W. Plummer, *Phys. Rev. B* **48**, 8119 (1993).
- ¹⁰F. Bechstedt and M. Scheffler, *Surf. Sci. Rep.* **18**, 145 (1993), and references therein.
- ¹¹L. J. Whitman, J. A. Stroschio, R. A. Dragoset, and R. J. Celotta, *Phys. Rev. Lett.* **66**, 1338 (1991); P. N. First, R. A. Dragoset, Joseph A. Stroschio, R. J. Celotta, and R. M. Feenstra, *J. Vac. Sci. Technol. A* **7**, 2868 (1989).
- ¹²L. J. Whitman, J. A. Stroschio, R. A. Dragoset, and R. J. Celotta, *Phys. Rev. B* **44**, 5951 (1991); *J. Vac. Sci. Technol. B* **9**, 770 (1991).
- ¹³S. Modesti, A. Falasca, M. Polentarutti, M. G. Betti, V. De Renzi, and C. Mariani, *Surf. Sci.* **447**, 133 (2000).
- ¹⁴M. G. Betti, V. Corradini, M. Sauvage-Simkin, and R. Pinchaux,

- Phys. Rev. B* **66**, 085335 (2002).
- ¹⁵G. Faraci, A. R. Pennisi, F. Gozzo, S. La Rosa, and G. Margaritondo, *Phys. Rev. B* **53**, 3987 (1996).
- ¹⁶K. M. Schirm, P. Soukiassian, P. S. Mangat, and L. Soonckindt, *Phys. Rev. B* **49**, 5490 (1994).
- ¹⁷N. J. Di Nardo, T. M. Wong, and E. W. Plummer, *Phys. Rev. Lett.* **65**, 2177 (1990).
- ¹⁸K. O. Magnusson and B. Reihl, *Phys. Rev. B* **40**, 5864 (1989); **40**, 5864 (1989).
- ¹⁹J. Hebenstreit, M. Heinemann, and M. Scheffler, *Phys. Rev. Lett.* **67**, 1031 (1991); J. Hebenstreit and M. Scheffler, *Phys. Rev. B* **46**, 10 134 (1992).
- ²⁰O. Pankratov and M. Scheffler, *Phys. Rev. Lett.* **71**, 2797 (1993); *Surf. Sci.* **287/288**, 584 (1993).
- ²¹A. Calzolari, C. A. Pignedoli, R. Di Felice, C. M. Bertoni, and A. Catellani, *Surf. Sci.* **454-456**, 207 (2000); A. Calzolari, C. A. Pignedoli, R. Di Felice, C. M. Bertoni, and A. Catellani, *ibid.* **491**, 265 (2001).
- ²²L. Gavioli, M. Padovani, E. Spiller, M. Sancrotti, and M. G. Betti, *Surf. Sci.* **532-535**, 666 (2003).
- ²³D. R. Lide, *CRC Handbook of Chemistry and Physics*, 76th ed. (CRC Press, Boca Raton, FL, 1995).
- ²⁴R. Wiesendanger, *Scanning Probe Microscopy and Spectroscopy: Methods and Applications* (Cambridge University Press, New York, 1994).
- ²⁵M. G. Betti, G. Bertoni, V. Corradini, S. Gardonio, C. Mariani, L. Gavioli, R. Belkou, and A. Taleb Ibrahim, *Surf. Sci.* **477**, 35 (2001).
- ²⁶S. D'Addato, P. Bailey, J. M.C. Thornton, and D. A. Evans, *J. Phys.: Condens. Matter* **10**, 2861 (1998).